

Two-dimensional spin-polarized states of Ag on Fe(100)

E. Vescovo

Institut für Festkörperforschung, Kernforschungsanlage Jülich, D-52425 Jülich, Germany

O. Rader

Berliner Elektronenspeicherring-Gesellschaft für Synchrotronstrahlung m.b.H., D-14195 Berlin, Germany

J. Redinger,* S. Blügel, and C. Carbone

Institut für Festkörperforschung, Kernforschungsanlage Jülich, D-52425 Jülich, Germany

(Received 20 June 1994; revised manuscript received 31 October 1994)

We present an experimental and theoretical investigation of the spin-dependent electronic structure of a Ag monolayer on Fe(100). By spin- and angle-resolved photoemission we identify several spin-polarized states of two-dimensional (2D) character and determine their band dispersion. The experimental results are compared with *ab initio* band-structure calculations. Three kinds of spin-polarized 2D states could be identified along the $\bar{\Gamma}-\bar{X}$ high-symmetry direction of the surface Brillouin zone: (i) 3d-derived Fe surface states which are only weakly modified by the Ag overlayer; (ii) Fe surface states with a substantial *sp* character which, upon adsorption of a Ag overlayer, hybridize with the Ag atoms and form interface states; (iii) Ag-induced spin-polarized interface states which are shared by both of the constituents of the interface atoms and do not have any counterpart at the clean Fe surface.

I. INTRODUCTION

The electronic states that are localized at the interface between two different materials are important in determining the magnetic properties of ultrathin films and multilayers.¹ For example, the magnetic structure of some rare-earth-transition metal multilayers,² consisting of ferromagnetic layers alternatively ordered in opposite directions, originates from the antiferromagnetic interface coupling between the two materials. In other interface systems, with only one magnetic component, the bonding at the interface induces a moment in the nonmagnetic material through spin-dependent electronic hybridization.³ Ferromagnetic order is thus attained in nonmagnetic transition-metal overlayers on Fe, primarily through the effect of *d-d* hybridization. The resulting magnetization is often sizable but it typically decays rapidly away from the interface on the scale of a few atomic layers.^{2,4}

In this paper we present an investigation of the electronic structure of a Ag overlayer on Fe(100), by combining spin- and angle-resolved photoemission with *ab initio* electronic-structure calculations. The moment locally induced on a noble metal at the interface with a 3d ferromagnet is theoretically expected to be quite small, because of the limited overlap between the *d* states of the two interface constituents. For instance, a magnetic moment of $0.06\mu_B$ is predicted for Ag on Fe(100).⁵ For the Fe atom underneath Ag the moment is expected to be $2.5\mu_B$, enhanced as compared to the bulk value ($2.2\mu_B$) but already reduced with respect to the value for Fe at a free surface ($2.9\mu_B$).⁵ On the other hand, the spin polarization induced on some electronic states of the noble metal by the spin-dependent bonding at the interface can persist over several layers. *Sp*-derived states in noble-

metal overlayers on a ferromagnetic substrate have been shown to be spin polarized up to film thicknesses of at least ten atomic layers.⁶ These states can be described as two-dimensional quantum-well states in the high coverage limit.⁷ Until now, the development of these polarized states with the overlayer thickness has been studied for Cu on Co(100) (Refs. 6 and 8) and for Ag on Fe(100).⁹ Although these states induce only a negligible magnetic moment in the noble metal, they are of great importance in magnetic multilayers because they mediate the long-range exchange interactions between the magnetic layers.

The main aim of this work is to determine the properties of the two-dimensional states initially formed at the interface between these two materials. In particular we examine how *sp*-derived Ag states contribute to form two-dimensional magnetic bands, which eventually develop into "quantum-well states" in thicker Ag films. By comparing the experimental data to *ab initio* electronic-structure calculations for Fe(100) and for 1 monolayer (ML) Ag on Fe(100) we identify "true" and spin-polarized interface states, i.e., magnetic states which are localized at the interface and shared by both of the constituents Fe and Ag. These states are found to originate either from particular Fe surface states or from the Ag overlayer. In the latter case, these states can be described as the precursors of the spin-polarized quantum-well states⁷ which develop in thicker Ag overlayers. Other two-dimensional states, derived from Fe surface states, are found instead to be only weakly modified by the presence of the overlayer.

II. EXPERIMENTAL RESULTS

The experiment has been performed at the storage ring BESSY with the spin- and angle-resolved photoemission

apparatus described elsewhere.¹⁰ As in Ref. 6 the geometry of the experiment has been modified in order to have a component of the electric-field vector perpendicular to the surface plane ($\theta_i = 30^\circ$ in normal emission condition). Photoemission spectra have been measured with photon energies between 40 and 80 eV on the TGM5-Undulator beamline.¹¹ Epitaxial Fe films have been deposited *in situ* on a Ag(100) single crystal at room temperature by *e*-beam evaporation.

The growth of Fe on Ag(100) has already been extensively characterized. While the early stage of growth is still somewhat controversial, it is well established that thick Fe films (10–30 ML) closely resemble the bcc structure of α -Fe.¹²

During the growth of the Fe layer a small amount of surface segregation of Ag takes place already at room temperature¹³ and can be further enhanced by annealing the sample above 200 °C. We have produced a Ag overlayer on a 10 ML Fe film by annealing the sample at 250 °C for about 40 min. The evolution of the system during this procedure is shown in Fig. 1 where the following photoemission spectra are shown: clean Ag(100) sample before (a) and after deposition of 10 ML Fe at room temperature (b) and during a sequence of five annealing steps at 250 °C for about 10 min each [Figs. 1(c)–1(g)]. In these spectra the Ag 4*d* band emission, above 4 eV binding energy, is well separated from the Fe 3*d*-derived states at lower binding energy. It is worth noticing that, at the photon energy used in this experiment, the Fe 3*p* Auger emission is degenerate with the Ag 4*d* valence emission. This Auger emission, together with the emission from some surface segregated Ag account for the broad feature below 4 eV binding energy in Fig. 1(b). The amount of Ag segregation depends on the

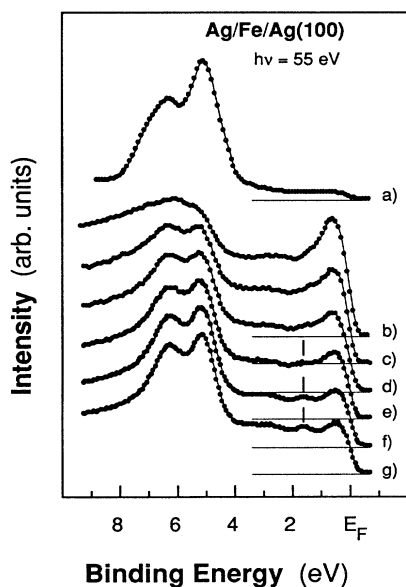


FIG. 1. Angle-resolved photoemission spectra of clean Ag(100) (a), 10 ML Fe on Ag(100) (b), and after each of the subsequent annealing steps of 10 min each at 250 °C (c)–(g). The spectra are measured with the sample at room temperature in normal emission condition at a photon energy of 55 eV.

Fe film thickness, because the segregation process is kinetically limited at room temperature. Upon annealing, the intensity of the Ag 4*d* emission is increased [Figs. 1(c)–1(f)] due to further segregation from the substrate. This procedure rapidly converges to a stable configuration where further annealing is no longer effective [compare spectra 1(f) and 1(g)].

The completion of a Ag layer on top of the Fe surface is accompanied by substantial changes in the valence-band region within 4 eV from the Fermi level. The normal emission spectra, at photon energies between 45 and 70 eV, show in particular the development of a new Ag-induced structure at 1.8 eV binding energy (marked in Fig. 1). The binding energy of this spectral feature corresponds to the one obtained after evaporation of a Ag monolayer onto an Fe(100) surface by Brookes, Chang, and Johnson.¹⁴ Thus the system prepared in this way consists of Ag (1 ML) / Fe (10 ML) / Ag(100) and is stable upon further heating and upon cooling to room temperature. The two-dimensional character of the overlayer is also confirmed by the absence of dispersion of the Ag 4*d* states in normal emission for varying energy. At the final stage of the sample preparation, we obtained a good low-energy electron diffraction pattern with a signal-to-background ratio improved with respect to the one of the Fe layer just deposited on Ag(100) substrate.

In order to investigate the two-dimensional electronic structure of the 1 ML Ag/Fe/Ag(100) system we have measured photoemission spectra varying the emission angle (Fig. 2). States with parallel wave vectors (k_{\parallel}) along the $\bar{\Gamma}$ - \bar{X} - $\bar{\Gamma}'$ high-symmetry direction of the surface Brillouin zone are sampled in these spectra. In this experimental geometry dipole selection rules dictate that the initial states are even with respect to reflection symmetry in the (010) Fe plane.

In Fig. 2 tick marks label the most prominent features. The Ag-induced structure, located at 1.8 eV binding energy for normal emission ($\bar{\Gamma}$), shifts towards lower binding energy as k_{\parallel} approaches \bar{X} , which is reached at about 20° off normal emission. Further increase of the emission angle (k_{\parallel} in the second surface Brillouin zone \bar{X} - $\bar{\Gamma}'$) forces this structure to shift backwards thus displaying a symmetric dispersion with respect to the two-dimensional zone boundary (\bar{X}).

In addition to this main structure, the off-normal spectra show two other interesting features. In the region near $\bar{\Gamma}$, the spectra display a peak at the Fermi level. This structure rapidly vanishes when the emission angle is increased. This behavior suggests that the state causing the peak at normal emission ($\bar{\Gamma}$) moves toward lower binding energies in the off-normal spectra and eventually crosses the Fermi level midway between $\bar{\Gamma}$ and \bar{X} . A third feature visible in the spectra is located at about 3 eV binding energy close to the zone boundary (\bar{X}). The structure is better observed experimentally in the second Brillouin zone.

A more detailed analysis of these states can be obtained from the spin-resolved photoemission spectra. These spectra are presented as a function of the emission angle in Fig. 3. The measurements have been performed in remanent magnetization after having magnetized the

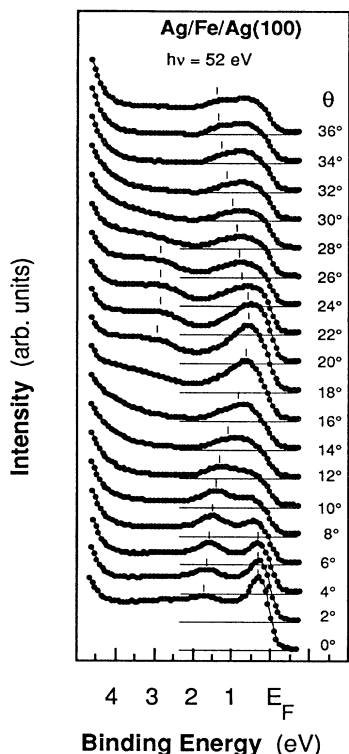


FIG. 2. Angle-resolved photoemission spectra of 1 ML Ag/10 ML Fe/Ag(100) as a function of the emission angle. Different electronic states with parallel wave vectors along the $\bar{\Gamma}$ - \bar{X} line of the two-dimensional surface Brillouin zone are selected as a function of the emission angle. In normal emission initial states at $\bar{\Gamma}(k_{\parallel}=0)$ are sampled. At 52 eV photon energy for a state at the Fermi level the first zone boundary ($\bar{X}, k_{\parallel}=1.09 \text{ \AA}^{-1}$) is reached at about 20° .

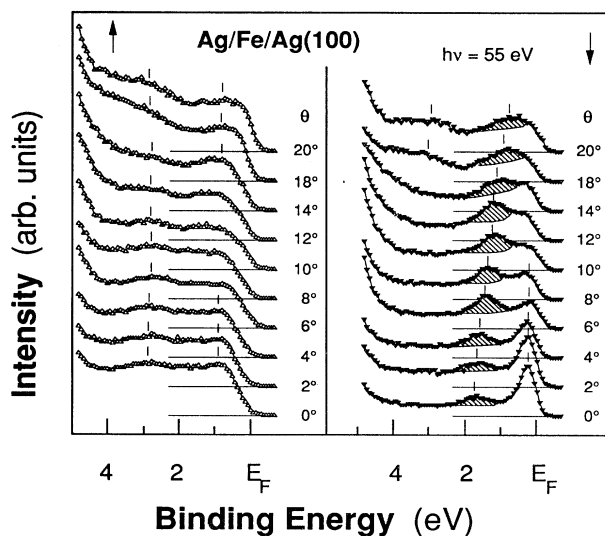


FIG. 3. Spin-resolved photoemission spectra from 1 ML Ag/10 ML Fe/Ag(100) as a function of the emission angle. Left panel: majority spectra; right panel: minority spectra. The shadowed structure in the minority spectra is the Ag-induced interface state discussed in the text.

sample along the in-plane Fe $\langle 001 \rangle$ direction, which was aligned to the spin-sensitive axis of the Mott spin detector. Several polarized features can be observed in the spectra. The spin-up spectra (left panel) present two rather broad structures, near 1 and 3 eV binding energy, respectively. These spectra do not show strong changes with varying emission angle. A much more interesting situation is instead observed in the spin-down channel (right panel). Here the spectra display a few features with a dispersive behavior. A spin-down peak (shadowed in Fig. 3), located at 1.8 eV binding energy at $\bar{\Gamma}$, moves to lower binding energy and reaches about 1 eV at \bar{X} . Clearly this feature corresponds to the two-dimensional Ag-induced peak already mentioned in the description of the spin-summed spectra (see Fig. 2). Another pronounced spin-down structure appears in the normal-emission spectrum near the Fermi level. Its intensity decreases for off-normal emission angles and practically vanishes for angles larger than 8° . Also the third structure observed in the spin-summed spectra turns out to be of minority character. Indeed a weak and broad peak appears in the spin-down channel close to \bar{X} at 3 eV binding energy.

In Fig. 4 the experimentally determined band dispersion outlines the results presented above (upper panel: spin-down; lower panel: spin-up). The data are presented in the repeated zone scheme. In the figure are also shown, as gray shadowed areas, those regions where surface projected Fe bulk states are obtained by our *ab initio* calculations which will be discussed in detail below. Two observed spin-down bands, near $\bar{\Gamma}$ close to E_F and near \bar{X} at 3 eV binding energy, are in the gaps of the Fe bulk spin-down band structure. Conversely, the spin-down

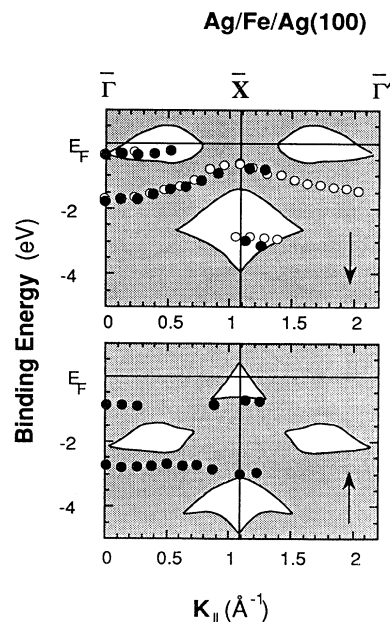


FIG. 4. Experimental determination of the energy dispersion $[E(k_{\parallel})]$ along the high symmetry line $\bar{\Gamma}$ - \bar{X} - $\bar{\Gamma}$ of the 2D Brillouin zone for 1 ML Ag/Fe/Ag(100). Upper panel: minority spin; lower panel: majority spin. The open points are derived from the spin-summed data (Fig. 2), while the closed ones are extracted from the spin-resolved spectra (Fig. 3).

band between 1–2 eV induced by the Ag overlayer as well as the experimentally observed spin-up states are degenerate with bulk states.

An examination of the lower panel of Fig. 4 clearly shows that all the structures that we have observed in the majority-spin spectra are degenerate with the bulk bands of the Fe substrate. This fact strongly complicates the interpretation of these features and prevents a unique assignment of the majority features to the calculated bands.

III. THEORETICAL RESULTS

In order to clarify the origin of the various spectral features we have performed first-principles calculations on the basis of the density-functional theory in the local-spin density approximation using the functional form of von Barth and Hedin¹⁵ with parameters after Moruzzi, Janak, and Williams.¹⁶ The density-functional equations are solved by the full-potential linearized augmented-plane-wave (FLAPW) method,¹⁷ which is known to be precise for open structures such as surfaces containing transition-metal atoms. Self-consistent calculations have been carried out for a nine-layer thick Fe(100) film, and a nine-layer thick 1 ML Ag/Fe(100) film consisting of a seven-layer Fe(100) film covered with one layer of Ag on each side of the Fe surface. The position of the Ag atoms were chosen in perfect registry with the substrate Fe atoms. The Ag-Fe interlayer spacing was chosen to be the average of their bulk lattice spacings and for the Fe-Fe interlayer spacings the bulk lattice spacing was used. The lattice parameters was chosen according to Ref. 16.

Although the film thickness taken into account is sufficient to determine the work function and structure reliably, the distinction of surface states or interface states from bulk projected bands or the observation of partial gaps in the band structure remain difficult. Therefore, we use thick films of 27 and 29 layers for Fe(100) and Ag/Fe(100), respectively, to analyze the band structure. The potential and density for the thick films were obtained by a stretching technique that makes use of the thinner slabs and bulk results. Although the calculations are not self-consistent enough for total energy purposes the bands are stable. The stability has been tested for various systems, among them Fe(100). We have started with a self-consistent nine-layer Fe(100) film, which has been stretched to a 15-layer slab. For this slab and for a self-consistently determined 15-layer slab the band structures have been compared. They turned out to be indistinguishable.

In Fig. 5 we present the results of the spin-polarized calculation for the 1 ML Ag/Fe(100) 29-layer slab [left panels: (a) and (b)] and for the Fe(100) 27-layer slab [right panels: (c) and (d)], respectively (upper panels: minority-spin; lower panels: majority-spin). To facilitate the comparison with the experimental results, only states with even symmetry are shown in these pictures. In Figs. 5(a) and 5(b) we have marked (with different symbols, whose meaning will be discussed below) the states, whose expectation value for the electron charge on the interface Ag and Fe atoms is more than 50%.

A first comparison between the experimental disper-

sion (Fig. 4: repeated-zone scheme) and the theoretical calculation [Fig. 5(a): reduced-zone scheme] reveals that all of the three minority features observed in the photoemission spectra are well reproduced in the calculated electronic structure. Indeed in the symmetry projected minority gap across the Fermi level there is a surface band which, starting at $\bar{\Gamma}$ at about 0.5 eV binding energy, moves towards E_F and crosses it midway from $\bar{\Gamma}$ to \bar{X} [squares in Fig. 5(a)]. Clearly this band can be identified with the peak experimentally observed near the Fermi level for small emission angles (Fig. 4). In Fig. 5(a), degenerate with the Fe projected bulk states, we found another minority band which at $\bar{\Gamma}$ is located at 1.8 eV below the Fermi level [empty squares in Fig. 5(a)]. Obviously this band corresponds to the Ag-induced states. Also in this case the dispersion experimentally observed for this minority structure along the $\bar{\Gamma}$ - \bar{X} high-symmetry

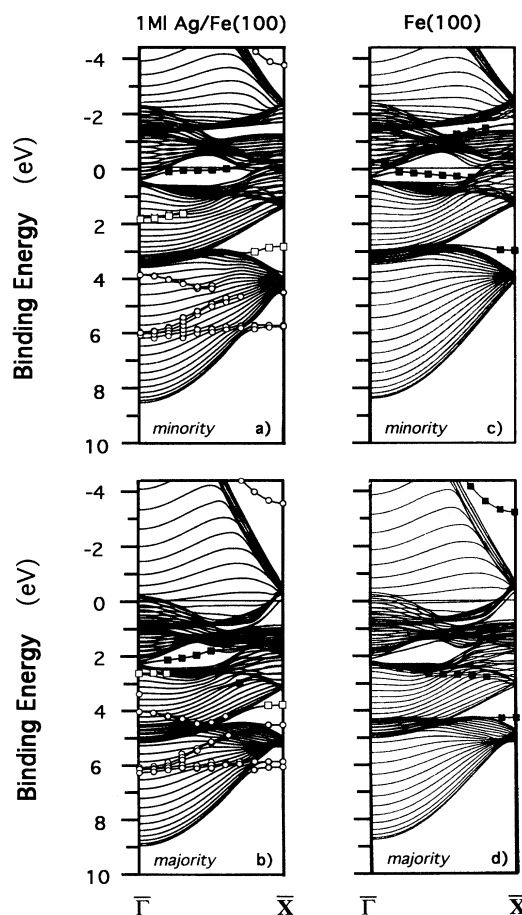


FIG. 5. Band-structure calculation for a 27-layer Fe(100) film covered on both sides with a Ag monolayer arranged in the pseudomorphic $p(1 \times 1)$ geometry (a) and (b) and for a 27-layer Fe(100) film (c) and (d) along $\bar{\Gamma}$ - \bar{X} . Only states along $\bar{\Gamma}$ - \bar{X} and with even symmetry with respect to the (010) Fe plane are shown in the pictures. Upper panel: minority bands; lower panel: majority bands. In both calculations various states are marked [Ag/Fe(100) full squares: Fe states; empty squares: interface states; empty circles: Ag states. Fe(100), full squares indicate surface states. For a precise definition see text].

direction fits to the one determined from the first-principles calculations. Finally, in the second minority gap located at about 3 eV binding energy close to \bar{X} lies a surface band [empty squares in Fig. 5(a)]. These states closely correspond to the broad minority structure experimentally observed at 3 eV binding energy in the region across the surface-zone boundary (\bar{X}). Notice that close to \bar{X} , in correspondence with the appearance in the minority spectra of the new peak, the majority spectra also display some minor changes in the structure at about 3 eV (see Fig. 3). This is probably related to the coming out, at higher binding energy, of the exchange-split majority counterpart of the minority peak located at 3 eV. Unfortunately, due to the short lifetime of the high binding energy features, the majority spectra at \bar{X} do not show clearly a new peak, at higher binding energy, separate from the one originating from the Fe majority bulk bands.

A deeper insight into the nature of these states can be gained by comparing the electronic structure of the system 1 ML Ag/Fe(100) [Figs. 5(a) and 5(b)] with the one for the bare Fe substrate [Figs. 5(c) and 5(d)]. In the Fe calculations surface related states are extracted according to the criteria that at least 50% of their weight must be distributed on the surface topmost layer (full squares). Already in the case of the uncovered substrate both Fe minority gaps mentioned before are filled with surface bands and upon absorption of the Ag monolayer both bands survive with only minor modifications in their energy dispersion. The minority surface band, which on the clean Fe(100) surface remains just below the Fermi level along all $\bar{\Gamma}$ - \bar{X} , is only slightly pushed up in the Ag/Fe(100) system and eventually crosses the Fermi level in the middle of the zone. Analogous considerations can be done for the minority band found in the calculation at about 3 eV binding energy close to \bar{X} in the s - d hybridization gap. Also in this case the energy dispersion of the corresponding Fe surface states is only weakly modified by the Ag overlayer. In spite of this close similarity in the behavior of these two surface bands, a more quantitative analysis of the calculation reveals some interesting differences.

For this purpose, the various 2D states already selected (i.e., more than 50% on the two Fe and Ag outermost atomic layers) have been divided according to one of the following additional criteria which define:

- (i) Fe states: if 90% or more of their interface charge (i.e., the part of their charge which is distributed on the two Fe and Ag interface species) is located on the Fe layer [full squares in Figs. 5(a) and 5(b)].
- (ii) Ag states: if 90% or more of their interface charge is located on the Ag layer [empty circles in Figs. 5(a) and 5(b)].
- (iii) Interface states: if their charge distributed on the two Fe and Ag interface species is comparable, having a difference less than 10% [empty squares in Figs. 5(a) and 5(b) (Ref. 18)].

On the clean Fe surface [Fig. 5(c)], the minority states just below the Fermi level have a very high degree of localization on the topmost Fe surface layer (more than 70% of the total electronic density), i.e., these states have

a pronounced d character. Consequently, we find a very weak interaction in with the Ag overlayer [full squares in Fig. 5(a): 2D-Fe states]. The direct comparison between Figs. 5(a) and 5(c) clearly shows that the main effect of the Ag overlayer is that of producing an entirely new minority band that we have therefore mentioned before as Ag-induced. The energy position of this band indicates that it derives from the Ag sp bands. Moreover we can now see that this band verifies the criteria for interface states [empty squares in Fig. 5(a): Fe-Ag interface states] so that a state belonging to this band is substantially shared between the two interface layers. This result is in good agreement with a previous analysis by Brookes, Chang, and Johnson¹⁴ on the basis of a FLAPW calculation.¹⁹ They find that these states are localized at the interface for more than 67%. From Fig. 5(a) it appears that also the other minority states in the s - d hybridization gap centered at about 3 eV close to \bar{X} are interface states. An examination of the corresponding Fe surface states reveals that these states are quite delocalized already in the case of the clean Fe(100) surface (only about 60% of their total electronic density is located on the surface layer), i.e., they have a substantial sp character. Upon Ag adsorption these states are then modified and transform into interface states [empty squares in Fig. 5(a): Fe-Ag interface state].

In Fig. 6 we compare the layer-resolved charge distribution of three particular states of the minority bands discussed above. The Fe state at 0.3 eV binding energy is extremely localized on the Fe-interface layer, its intensity decreasing abruptly both inside the Fe substrate and in the Ag overlayer [Fig. 6(a)]. Instead, the Ag-induced state is more delocalized. At 1 ML Ag coverage, it forms an interface state which considerably extends in the Fe substrate. Nevertheless a significant part of this state is also distributed into the vacuum region [Fig. 6(b)]. This fact suggests that its nature could be profoundly modified by further Ag deposition. Finally, the third state considered at 2.8 eV binding energy at \bar{X} is a clear interface state derived from the corresponding Fe surface state. This state is in fact more concentrated at the interface [Fig. 6(c)]. Further support to this view comes from the observation that bulk Ag also has a symmetry projected gap very close to this band so that presumably these states will remain interface states also for thicker Ag layers.

As already mentioned, the Ag-induced interface states are particularly interesting due to their role in the magnetic coupling of Ag-based magnetic multilayers. In this case it is also interesting to analyze their layer distribution in other points along the $\bar{\Gamma}$ - \bar{X} line. Our calculations prove that in the region near $\bar{\Gamma}$, these states are nearly equally distributed between the top Fe layer and the Ag overlayer. Moving from $\bar{\Gamma}$ towards \bar{X} (or also towards \bar{M} , not shown in Fig. 5) the center of the electron density related to these states moves away from the interface. In the second half of $\bar{\Gamma}$ - \bar{X} (or $\bar{\Gamma}$ - \bar{M}) these states acquire the character of Fe resonances with increasing weight inside the Fe layers.

Moreover, it can be noticed in Fig. 5 that the two-dimensional Ag monolayer states are confined at binding

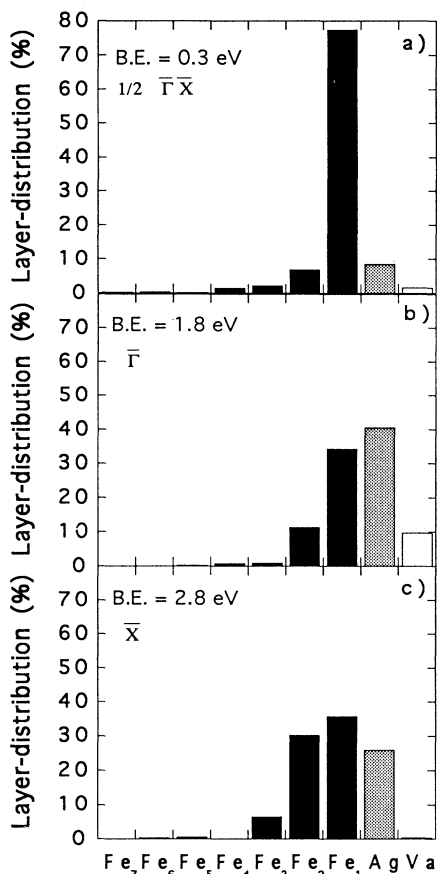


FIG. 6. Layer-resolved charge distribution for three representative minority states of the 1 ML Ag/Fe(100). The Fe layers are shown in black, the Ag in gray, and the vacuum in white.

energies between 3.5 and 6 eV (empty circles: Ag states). Similar calculations of the band structure for bulk Ag determine the position of the Ag d bands at binding energies between 3.2 and 6.5 eV.¹⁵ The reduction of the d -band width is attributed to the reduced coordination number of the Ag atoms in the monolayer. As a final remark we would like to point out that there is an excellent agreement between the calculation and the experiment in the first 3.5 eV binding energy region. This suggests that the system Ag/Fe(100) should be one in which the ideal geometry postulated in the calculations is to a great ex-

perimentally realized for the real system. However, the agreement becomes less satisfactory for the Ag $4d$ bands which in the calculations are located at about 0.5 eV lower binding energy than the experimental observations.

To conclude the analysis of our calculations, we mention that another interesting feature is observed in the empty part of the electronic states. On the Fe surface in the gap close to \bar{X} there are also Fe surface states. These states have a considerably high exchange splitting so that a majority state at about 3.2 eV above E_F at \bar{X} is visible in Fig. 5(d) but its minority counterpart is not [Fig. 5(c)]. Upon Ag deposition this Fe surface band is replaced by a Ag surface band. The exchange splitting of these Ag states is much reduced ($\Delta E_{ex} = 0.21$ eV at \bar{X}) and correspondingly we find that indeed these states are highly localized on the Ag layer [empty circles in Figs. 5(a) and 5(b)].

IV. CONCLUSIONS

In conclusion, we have shown how sp -derived Ag states contribute to form two-dimensional magnetic bands. By comparing the experimental data to FLAPW calculations for thin films of Fe(100) and 1 ML Ag on Fe(100), we have identified various types of 2D and spin-polarized electronic states, among them, Ag-induced magnetic states which are localized at the interface and shared by both of the constituent interface atoms. These states have no counterpart on the clean Fe surface and can be described as the precursors of the polarized quantum-well states which eventually develop in thicker Ag films. Other two-dimensional states, derived from Fe surface states, are instead found either negligibly modified or changed into interface states by the presence of the Ag overlayer. The distinct behavior of these states is traced back to their different degree of localization at the Fe surface.

ACKNOWLEDGMENTS

We wish to thank Professor W. Eberhardt and Professor W. Gudat for their interest and support in this work. Two of us (J.R. and S.B.) are thankful to M. Weinert for his contribution building up the stretching potential scheme and to S. Handschuh for her assistance performing the calculations. We acknowledge that the computations were performed on Cray computers of the Forschungszentrum Jülich and the German supercomputer center (HLRZ).

*Permanent address: Institut für Technische Elektrochemie, Technische Universität Wien, Getreidemarkt 9, A-1060 Wien, Austria.

¹A. J. Freeman and R. Wu, *J. Magn. Magn. Mater.* **100**, 497 (1991); M. Weinert and S. Blügel, in *Magnetic Multilayers*, edited by L. H. Bennett and R. E. Watson (World Scientific, Singapore, 1993).

²Z. S. Shan, D. J. Selmyer, S. S. Jaswal, Y. J. Wang, and J. X. Shen, *Phys. Rev. Lett.* **63**, 449 (1989); M. Taborrelli, R. Allenspach, G. Boffa, and M. Landolt, *ibid.* **56**, 2869 (1986); C.

Carbone and E. Kisker, *Phys. Rev. B* **36**, 1280 (1987).

³W. Weber, D. A. Wesner, G. Güntherodt, and U. Linke, *Phys. Rev. Lett.* **66**, 942 (1991); O. Rader, C. Carbone, W. Clemens, E. Vescovo, S. Blügel, W. Eberhardt, and W. Gudat, *Phys. Rev. B* **45**, 13 823 (1992); T. Kachel, W. Gudat, C. Carbone, E. Vescovo, U. Alkemper, S. Blügel, and W. Eberhardt, *ibid.* **46**, 12 888 (1992); D. Hartmann, W. Weber, A. Rampe, S. Popovic, and G. Güntherodt, *ibid.* **48**, 16 837 (1993); O. Rader, E. Vescovo, J. Redinger, S. Blügel, C. Carbone, W. Eberhardt, and W. Gudat, *Phys. Rev. Lett.* **72**, 2247 (1994).

- ⁴K. Totland, P. Fuchs, J. C. Groebli, and M. Landolt, *Phys. Rev. Lett.* **70**, 2487 (1993).
- ⁵A. J. Freeman, C. L. Fu, S. Ohnishi, and M. Weinert, in *Polarized Electrons in Surface Physics*, edited by R. Feder (World Scientific, Singapore, 1985).
- ⁶C. Carbone, E. Vescovo, O. Rader, W. Gudat, and W. Eberhardt, *Phys. Rev. Lett.* **71**, 2805 (1993).
- ⁷J. Ortega and F. J. Himpsel, *Phys. Rev. Lett.* **69**, 844 (1992); J. Ortega, F. J. Himpsel, G. J. Mankey, and R. F. Willis, *Phys. Rev. B* **47**, 1540 (1993).
- ⁸K. Garrison, Y. Chang, and P. D. Johnson, *Phys. Rev. Lett.* **71**, 2801 (1993).
- ⁹N. V. Smith, N. B. Brookes, Y. Chang, and P. D. Johnson, *Phys. Rev. B* **49**, 332 (1994).
- ¹⁰E. Kisker and C. Carbone, in *Angle-resolved Photoemission*, edited by S. Kevan (Elsevier, Amsterdam, 1992).
- ¹¹W. Peatman, C. Carbone, W. Gudat, W. Heinen, P. Kuske, J. Pflüger, F. Schäfers, and T. Schroeter, *Rev. Sci. Instrum.* **60**, 1445 (1989).
- ¹²H. Li, Y. S. Li, J. Quinn, D. Tian, J. Sokolov, F. Jona, and P. M. Marcus, *Phys. Rev. B* **42**, 9195 (1990).
- ¹³B. T. Jonker, K.-H. Walker, E. Kisker, G. A. Prinz, and C. Carbone, *Phys. Rev. Lett.* **57**, 142 (1986).
- ¹⁴N. B. Brookes, Y. Chang, and P. D. Johnson, *Phys. Rev. Lett.* **67**, 354 (1991). The position of this peak is a critical test on the thickness of the Ag overlayer. As shown in Ref. 14, at two monolayers it is shifted to 1 eV binding energy, and at three it is at 0.3 eV from the Fermi level. Moreover notice that our spectrum for 1 ML Ag [Fig. 1(g)] shows a more pronounced emission near the Fermi level than the one reported by Brookes *et al.* This difference is due to the different light incidence used in the two experiments: 30° incidence in our case and 70° incidence in their case.
- ¹⁵U. von Barth and L. Hedin, *J. Phys. C* **5**, 1629 (1972).
- ¹⁶V. L. Moruzzi, J. F. Janak, and A. R. Williams, *Calculated Electronic Properties of Metals* (Pergamon, New York, 1978).
- ¹⁷E. Wimmer, H. Krakauer, M. Weinert, and A. J. Freeman, *Phys. Rev. B* **24**, 864 (1981); M. Weinert, E. Wimmer, and A. J. Freeman, *ibid.* **26**, 4571 (1981).
- ¹⁸These three conditions do not cover all the possible 2D states according to our definition of 50% or more of their total charge confined in the two interface layers. On the other side it has the advantage of excluding ambiguous cases where the distinction between Fe states, interface states, and Ag states would become only a matter of convention.
- ¹⁹S. Ohnishi, M. Weinert, and A. J. Freeman, *Phys. Rev. B* **30**, 36 (1984).